Electron scattering by atomic sodium: $3^2S - 3^2S$ and $3^2S - 3^2P$ cross sections at 10 to 100 eV

Igor Bray, Dmitry A. Konovalov, and Ian E. McCarthy
Electronic Structure of Materials Centre, School of Physical Sciences,
The Flinders University of South Australia,
G.P.O. Box 2100, Adelaide 5001, Australia
(Received 13 May 1991)

A coupled-channel optical method for electron-atom scattering is applied to electron-sodium scattering at energies of 10, 20, 22.1, 40, 54.4, and 100 eV. The 3^2S, 3^2P, and 3^2D channels are coupled explicitly whereas the rest of the one-electron excited states of the atom are taken into account via the *ab initio* complex nonlocal polarization potential. The $3^2S - 3^2S$ and $3^2S - 3^2P$ differential cross sections are found to be in good agreement with the recent experiments of Lorentz and Miller (unpublished). The effect of the polarization potential does not change the qualitative results of a standard coupled-channel calculation, but improves agreement with the experiment. Integrated and total cross sections are also presented.

PACS number(s): 34.80.Bm, 34.80.Dp 34.80Nz

I. INTRODUCTION

For the past two decades electron scattering on atomic sodium has been greatly studied by a number of experimental and theoretical groups. This is due to the fact that sodium is a relatively simple target for both experimentalists and theorists, and there are still some unresolved discrepancies between theory and some experimental data. We would like to apply our recently developed method, for calculation of electron-atom scattering phenomena, to electron scattering from atomic sodium in an attempt to resolve some of these discrepancies.

We use the coupled-channel optical (CCO) method which is an *ab initio* approach to electron-atom scattering. It treats a finite set of scattering channels (P space) explicitly via the coupled-channel formalism, whilst the rest of the channels (Q space), including the target continuum, are taken into account indirectly through a complex nonlocal polarization potential. This potential, together with the first-order potential of the explicitly treated channels, forms the optical potential. We use the notations nCC and nCCO for calculations that have the lowest n target states in P space; the latter treats the Q space via the polarization potential, whereas the former leaves it out completely.

The strength of the CCO approach to electron-atom scattering is that it treats the complete set of target states up to convergence [1]. The effect of higher excited states on scattering within a set of low-lying states can be seen by comparing corresponding nCCO and nCC calculations. Furthermore, the polarization potential may be tested internally by comparing nCCO with n'CCO calculations, for $n' > n$ [2].

Our CCO approach has proved to be very successful in the description of electron-hydrogen elastic scattering at energies ranging from 0.5 to 30 eV [3] and elastic and inelastic scattering from 30 to 400 eV [4]. We have recently expanded our CCO theory to incorporate alkali atoms which we treat by the one electron above the frozen-core model. This theory has worked extremely well in the description of elastic scattering from sodium at 20 to 150 eV [5], where we did a series of 1CCO (P space contains 3^2S only) calculations.

For hydrogen the complete set of target states is known exactly. However this is not so for any other atom, and so approximations must be made to describe their structure. For alkali atoms we use the one-configuration self-consistent-field Hartree-Fock method to describe the ground state of the atom [6]. This approximation works very well for these atoms, see, for example, Ref. [7]. The complete set of the one-electron excited target states, including the continuum, is found by solving the one-electron Schrödinger equation with the frozen-core Hartree-Fock potential [8]. This is also a very good approximation as the effects of core excitation on scattering have been found to be negligible [9].

The aim of this paper is to use our recently developed theory [3, 5] to calculate the $3^2S - 3^2S$ and the $3^2S - 3^2P$ cross sections at a range of intermediate energies in an attempt to resolve some of the discrepancies between measurements by different experimental groups. In Sec. II we present the final equations of our CCO method, as the complete derivation of the theory may be found in McCarthy and Stelbovics [10] and Bray, Konovalov, and McCarthy [3, 5].

In Sec. III we present the results of 3CCO and 3CC (P space contains 3^2S, 3^2P, and 3^2D) calculations for projectile energies of 10, 20, 22.1, 40, 54.4, and 100 eV (Tables I – III). We compare these results with the measurements of elastic (Fig. 1) and inelastic (Fig. 2) differential cross sections of Lorentz and Miller [11], Srivastava and Vušković [12], and the Flinders University experimental group [13–16]. We find that agreement with the measurements of Lorentz and Miller and Srivastava and Vušković, which are in disagreement with the measurements of the Flinders group, is very good at all energies. In Table

III we also compare the total cross sections calculated via the optical theorem with the recent measurements of Kwan *et al.* [17], and find excellent agreement.

II. THE CCO METHOD FOR ALKALI ATOMS

To get the one-electron wave functions $\psi_j(\mathbf{r})$ of an alkali atom we solve the self-consistent-field Hartree-Fock equations [6] for the ground state of the atom A:

$$(K + v^{\mathrm{HF}} - \varepsilon_j)\,\psi_j(\mathbf{r}) = 0, \quad j \in A \tag{1}$$

where

$$v^{\mathrm{HF}}\psi_j(\mathbf{r}) = \left(-\frac{Z}{r} + 2\sum_{\psi_{j'}\in A}\int d^3r' \frac{|\,\psi_{j'}(\mathbf{r}')\,|^2}{|\,\mathbf{r}-\mathbf{r}'\,|}\right)\psi_j(\mathbf{r}) - \sum_{\psi_{j'}\in A}\int d^3r' \frac{\psi^*_{j'}(\mathbf{r}')\psi_j(\mathbf{r}')}{|\,\mathbf{r}-\mathbf{r}'\,|}\psi_{j'}(\mathbf{r}). \tag{2}$$

To get the complete set of one-electron excited target states we use the frozen-core Hartree-Fock approximation [8],

$$(K + v^{\mathrm{FC}} - \epsilon_j)\,\phi_j(\mathbf{r}) = 0, \quad j \notin C, \tag{3}$$

where

$$v^{\mathrm{FC}}\phi_j(\mathbf{r}) = \left(-\frac{Z}{r} + 2\sum_{\psi_{j'}\in C}\int d^3r' \frac{|\,\psi_{j'}(\mathbf{r}')\,|^2}{|\,\mathbf{r}-\mathbf{r}'\,|}\right)\phi_j(\mathbf{r}) - \sum_{\psi_{j'}\in C}\int d^3r' \frac{\psi^*_{j'}(\mathbf{r}')\phi_j(\mathbf{r}')}{|\,\mathbf{r}-\mathbf{r}'\,|}\psi_{j'}(\mathbf{r}), \tag{4}$$

and where the notation C indicates the set of frozen-core states. For sodium we take the core to be $1s^22s^22p^6\,{}^1S$.

As the target atom is described by the independent particle model that has one electron above a frozen core, all matrix elements in the Lippman-Schwinger equation, which describes the scattering, are reduced to two-electron matrix elements [10]. This integral equation for the T matrix, which depends on the total spin S, is

$$\langle \mathbf{k}\phi_i \mid T^S \mid \phi_{i_0}\mathbf{k}_0\rangle = \langle \mathbf{k}\phi_i \mid V_Q^S \mid \phi_{i_0}\mathbf{k}_0\rangle + \sum_{\phi_{i'}\in P}\int d^3k' \frac{\langle \mathbf{k}\phi_i \mid V_Q^S \mid \phi_{i'}\mathbf{k}'\rangle}{(E^{(+)} - \epsilon_{i'} - k'^2/2)}\langle \mathbf{k}'\phi_{i'} \mid T^S \mid \phi_{i_0}\mathbf{k}_0\rangle, \tag{5}$$

where the projectile with momentum $\mathbf{k}_0$ is incident on the target with the valence electron in state ϕ_{i_0} above the frozen core, and where $E = \epsilon_{i_0} + k_0^2/2$ is the on-shell energy. Writing the coordinate space-exchange operator as P_r the matrix elements of V_Q^S are given by [10]

$$\langle \mathbf{k}\phi_i \mid V_Q^S \mid \phi_{i'}\mathbf{k}'\rangle = \langle \mathbf{k}\phi_i \mid v^{\mathrm{FC}} + v_{12}[1 + (-1)^S P_r] \mid \phi_{i'}\mathbf{k}'\rangle + (-1)^S\langle \mathbf{k}\phi_i \mid (\epsilon_i + \epsilon_{i'} - E)P_r \mid \phi_{i'}\mathbf{k}'\rangle - \delta_{ii'}\sum_{\psi_j\in C}\langle \mathbf{k}\psi_j \mid (2\varepsilon_j - E)P_r \mid \psi_j\mathbf{k}'\rangle + \langle \mathbf{k}\phi_i \mid V_Q + (-1)^S V_Q P_r \mid \phi_{i'}\mathbf{k}'\rangle, \tag{6}$$

where v^{FC} is the projectile-core potential and v_{12} is the projectile-valence electron potential. The channel space is divided into two parts: P space and Q space. The channels in P space are coupled explicitly in (5), whereas the Q-space channels form the complex nonlocal polarization potential V_Q in (6). The details of the calculation of the polarization-potential matrix elements may be found in Refs. [3] and [5].

TABLE I. Elastic differential cross sections (a_0^2 sr^{-1}) calculated using the 3CCO model at a range of energies. Square brackets denote powers of 10.

	E (eV)					
θ (deg)	10.0	20.0	22.1	40.0	54.4	100.0
0	8.06[2]	8.02[2]	7.01[2]	4.95[2]	4.64[2]	2.85[2]
5	4.39[2]	2.71[2]	2.49[2]	1.45[2]	1.02[2]	5.92[1]
10	1.85[2]	8.10[1]	7.19[1]	3.84[1]	2.90[1]	1.99[1]
15	7.14[1]	2.56[1]	2.25[1]	1.26[1]	1.06[1]	8.16
20	2.64[1]	8.41	7.37	4.60	4.41	4.06
25	9.40	2.76	2.43	1.87	2.21	2.52
30	3.27	8.80[-1]	7.81[-1]	9.87[-1]	1.45	1.80
35	1.12	2.49[-1]	2.46[-1]	7.50[-1]	1.17	1.35
40	4.16[-1]	1.05[-1]	1.49[-1]	7.41[-1]	1.04	1.04
45	1.97[-1]	1.57[-1]	2.27[-1]	7.94[-1]	9.58[-1]	8.13[-1]
50	1.45[-1]	2.91[-1]	3.72[-1]	8.47[-1]	8.88[-1]	6.42[-1]
60	1.85[-1]	5.89[-1]	6.60[-1]	8.76[-1]	7.44[-1]	4.11[-1]
70	2.79[-1]	7.67[-1]	8.08[-1]	7.78[-1]	5.74[-1]	2.59[-1]
80	3.88[-1]	7.80[-1]	7.87[-1]	5.82[-1]	3.80[-1]	1.39[-1]
90	4.76[-1]	6.62[-1]	6.45[-1]	3.49[-1]	1.89[-1]	5.31[-2]
100	5.06[-1]	4.70[-1]	4.41[-1]	1.48[-1]	4.94[-2]	2.17[-2]
110	4.55[-1]	2.72[-1]	2.44[-1]	4.64[-2]	8.58[-3]	6.87[-2]
120	3.42[-1]	1.37[-1]	1.17[-1]	9.15[-2]	1.07[-1]	2.00[-1]
130	2.16[-1]	1.15[-1]	1.02[-1]	3.00[-1]	3.56[-1]	3.98[-1]
140	1.23[-1]	2.17[-1]	2.09[-1]	6.45[-1]	7.27[-1]	6.27[-1]
150	8.24[-2]	4.12[-1]	4.04[-1]	1.06	1.15	8.48[-1]
160	7.98[-2]	6.34[-1]	6.26[-1]	1.45	1.55	1.02
170	9.38[-2]	8.06[-1]	7.98[-1]	1.73	1.84	1.14
180	9.98[-2]	8.71[-1]	8.64[-1]	1.84	1.97	1.21

III. RESULTS AND DISCUSSION

Equation (5) is solved at a range of projectile energies ($k_0^2/2$). We take P space to contain 3^2S, 3^2P, and 3^2D as the 3^2S–3^2P and 3^2S–3^2D generalized oscillator strengths are the highest for scattering from the ground state [18]. This indicates that the 3^2P and 3^2D channels have the strongest coupling to the entrance channel 3^2S.

The strength of the CCO approach is that convergence, by the number of states in P space, may be tested internally. This convergence has been achieved when the corresponding results of an n'CCO calculation are the same as that of an nCCO calculation with $n' > n$. For sodium this can be done by comparing the elastic cross sections of the 1CCO calculation [5] with the corresponding results of our 3CCO calculations. Both of these yield much the same results. The fact that the polarization potential in the 1CCO calculations can reproduce the very strong dipole coupling ($3^2S - 3^2P$) that is explicitly in P space of our 3CCO calculations suggests that the higher excited states will also be suitably treated by our polarization potential.

The major discrepancy between theory and experiment for electron scattering on atomic sodium is between the absolute measurements of the Flinders University group [13–16] and the 4CC calculations of Mitroy, McCarthy, and Stelbovics [9] at intermediate and backward angles. As the core-excitation effects were found to be negligible [9] it was hoped that the discrepancies may be resolved

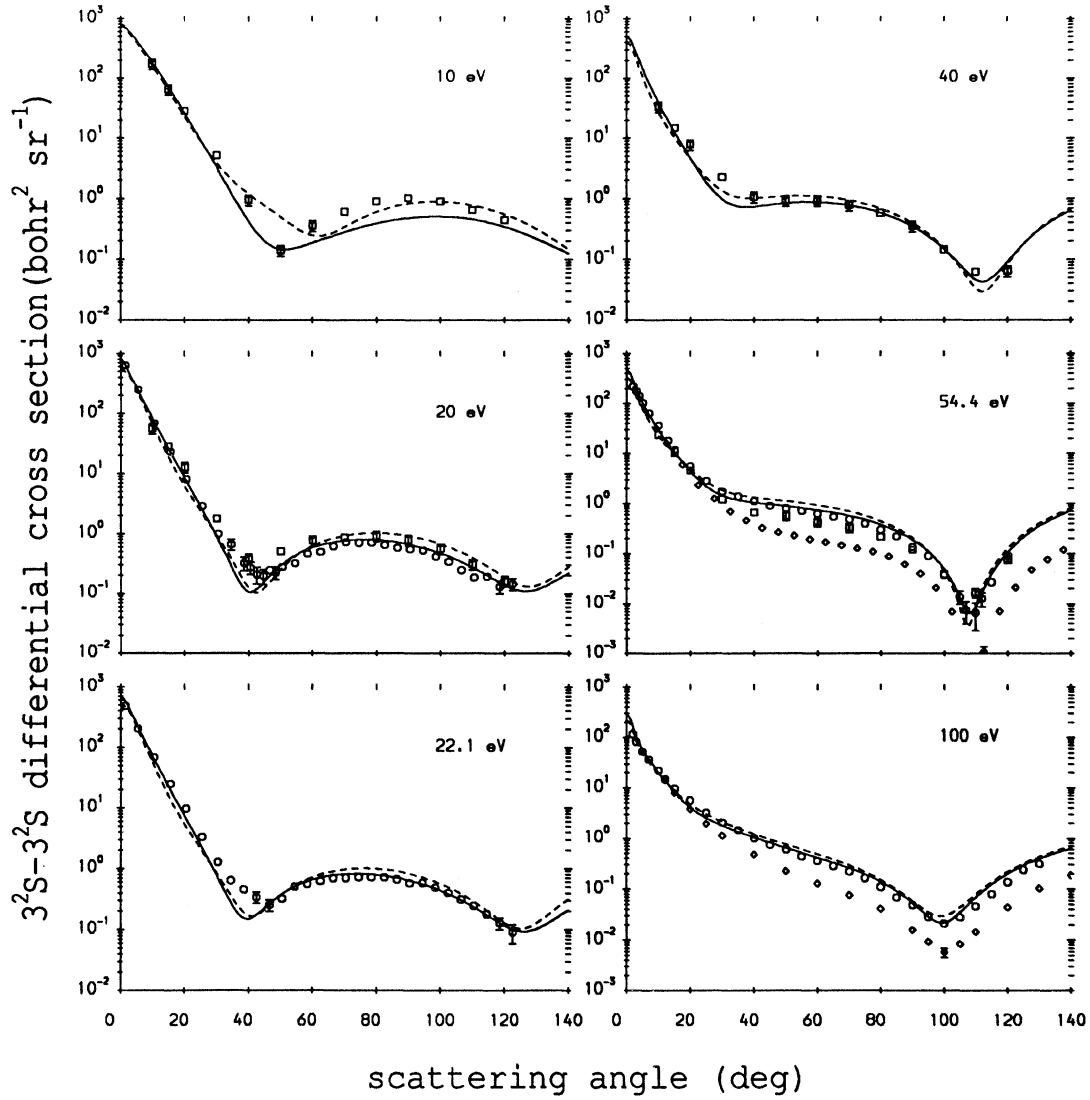

FIG. 1. Elastic differential cross sections for electron scattering on atomic sodium. The solid line is the 3CCO calculation and the dashed line is the 3CC calculation where the coupled channels are 3^2S, 3^2P, and 3^2D. The experiments of Lorentz and Miller [11] are denoted by o. Those of Srivastava and Vušković [12] are denoted by □. The measurements of the Flinders University group at 54.4 eV [16] and 100 eV [13] are denoted by ◇. All measurements have been normalized to the 3CCO estimates of σ_{3s} given in Table III. Error bars are only plotted if they are larger than the size of the symbol denoting the experiment.

by taking into account the complete set of one-electron excited target states. This proved to be not the case.

A. Elastic differential cross sections

In Fig. 1 we present the 3CC and 3CCO calculations together with available experimental data for the elastic scattering at a range of energies. Quantitative results are presented in Tables I and III. The measurements of Lorentz and Miller [11] are relative and have been normalized to the theoretical estimates for the integrated elastic cross section σ_{3s} of Mitroy, McCarthy, and Stelbovics [9]. The measurements of Srivastava and Vušković [12] are also relative, but they have been normalized to their estimate of σ_{3s} which have large error bounds. Accordingly, for plotting, we have renormalized their differential cross sections to our 3CCO estimates for σ_{3s} given in Table III.

Comparing 3CC with 3CCO it is evident that the effect of the polarization potential on elastic scattering is quite small, but improves agreement with experiment. The discrepancy with the Flinders group measurements at 54.4 and 100 eV cannot be resolved by the addition of the polarization potential. However the recent relative experiments by Lorentz and Miller [11] at these energies are in very good agreement with our 3CCO results. In general, the agreement between the 3CCO calculations and the measurements of Lorentz and Miller [11] and

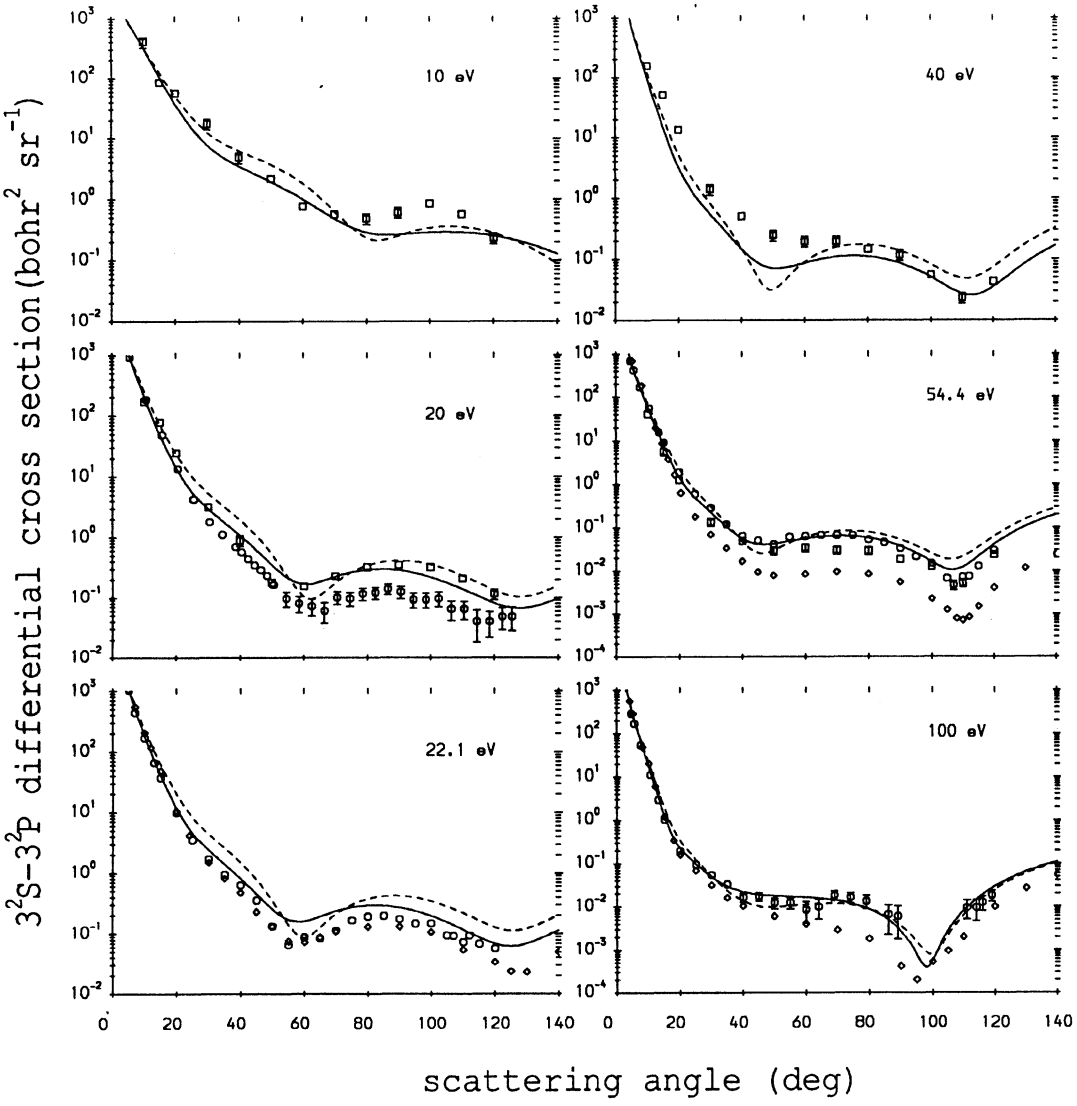

FIG. 2. $3\,^2S-3\,^2P$ differential cross sections for electron scattering on atomic sodium. The solid line is the 3CCO calculation and the dashed line is the 3CC calculation where the coupled channels are $3\,^2S$, $3\,^2P$, and $3\,^2D$. The experiments of Lorentz and Miller [11] are denoted by o and have been normalized to the 3CCO estimates of σ_{3p} given in Table III. Those of Srivastava and Vušković [12] are denoted by □. The measurements of the Flinders University group at 22.1 eV [15] and other energies [14] are denoted by ◇. Error bars are only plotted if they are larger than the size of the symbol denoting the experiment.

TABLE II. $3^2S - 3^2P$ differential cross sections (a_0^2 sr^{-1}) calculated using the 3CCO model at a range of energies. Square brackets denote powers of 10.

	E (eV)					
θ (deg)	10.0	20.0	22.1	40.0	54.4	100.0
0	1.61[3]	4.84[3]	5.50[3]	1.16[4]	1.67[4]	3.20[4]
5	9.27[2]	1.10[3]	1.06[3]	7.34[2]	5.46[2]	2.65[2]
10	3.19[2]	2.04[2]	1.82[2]	9.20[1]	5.79[1]	1.69[1]
15	1.05[2]	4.78[1]	4.08[1]	1.51[1]	7.82	1.23
20	3.72[1]	1.40[1]	1.15[1]	3.24	1.42	2.24[-1]
25	1.53[1]	5.61	4.57	1.14	4.90[-1]	9.66[-2]
30	7.82	2.96	2.39	5.57[-1]	2.24[-1]	4.90[-2]
35	4.91	1.78	1.39	2.84[-1]	1.04[-1]	2.96[-2]
40	3.50	1.07	8.10[-1]	1.46[-1]	5.49[-2]	2.20[-2]
45	2.61	6.25[-1]	4.52[-1]	8.73[-2]	4.09[-2]	1.91[-2]
50	1.94	3.52[-1]	2.55[-1]	7.06[-2]	4.18[-2]	1.78[-2]
60	1.00	1.69[-1]	1.62[-1]	8.65[-2]	5.54[-2]	1.64[-2]
70	4.83[-1]	2.24[-1]	2.36[-1]	1.09[-1]	6.35[-2]	1.38[-2]
80	2.86[-1]	2.91[-1]	2.93[-1]	1.10[-1]	5.70[-2]	8.71[-3]
90	2.65[-1]	2.85[-1]	2.72[-1]	8.55[-2]	3.70[-2]	2.69[-3]
100	2.87[-1]	2.18[-1]	1.97[-1]	5.04[-2]	1.59[-2]	5.52[-4]
110	2.87[-1]	1.37[-1]	1.17[-1]	2.70[-2]	1.20[-2]	8.21[-3]
120	2.52[-1]	8.08[-2]	6.92[-2]	3.51[-2]	4.01[-2]	2.95[-2]
130	1.92[-1]	6.75[-2]	6.93[-2]	8.32[-2]	1.05[-1]	6.48[-2]
140	1.26[-1]	9.64[-2]	1.14[-1]	1.65[-1]	2.00[-1]	1.09[-1]
150	7.22[-2]	1.52[-1]	1.86[-1]	2.66[-1]	3.07[-1]	1.57[-1]
160	3.86[-2]	2.14[-1]	2.59[-1]	3.62[-1]	4.05[-1]	1.99[-1]
170	2.24[-2]	2.60[-1]	3.15[-1]	4.28[-1]	4.72[-1]	2.28[-1]
180	1.75[-2]	2.78[-1]	3.38[-1]	4.50[-1]	4.95[-1]	2.37[-1]

those of Srivastava and Vušković [12] is very good for all energies.

B. $3^2S - 3^2P$ differential cross sections

In Fig. 2 we present the 3CC and 3CCO calculations together with available experimental data for the 3^2S-3^2P scattering. Quantitative results are presented in Tables II and III. For this transition only the measurements of Lorentz and Miller [11] are treated as relative and are renormalized accordingly as above.

Comparing 3CC with the 3CCO results we see that the effect of the polarization potential on $3^2S - 3^2P$ scattering is greater than that on the elastic scattering. The discrepancy between experiment and theory at 22.1 eV has been essentially resolved by the addition of the polarization potential. In general the agreement with experiment is considerably improved by the addition of the polarization potential at all energies.

One of the advantages of comparing theory against experiment at a range of energies is that one can examine the consistency of the results. For example, at first glance the agreement between the theory and experiment at 40 eV is disappointing. The disagreement at around 50°, where the theory predicts a local minimum, is quite large. However at both adjacent energies of 22.1 and 54.4 eV both the experiments and theory do have this local minimum and are in good agreement with each other. This makes us feel more confident with our results at 40 eV.

TABLE III. Integrated 3^2S-3^2S (σ_{3s}), 3^2S-3^2P (σ_{3p}), and total (σ_t) cross sections calculated using the 3CCO model at a range of energies. The experimental data of Srivastava and Vušković [12] are denoted by σ^a, that of Buckman and Teubner [14] by σ^b, that of Kasdan, Miller, and Bederson [19] by σ^c, and that of Kwan *et al.* [17] by σ^d.

	E (eV)					
σ (πa_0^2)	10.0	20.0	22.1	40.0	54.4	100.0
σ_{3s}	20.3	11.3	10.6	7.22	6.06	4.27
σ_{3s}^a	48.9±14.7	15.9 ± 4.8		12.5±3.8	6.14±1.84	
σ_{3p}	36.7	34.4	33.2	27.2	22.2	12.8
σ_{3p}^a	36.0±10.8	33.0 ± 1.0		24.8±7.4	21.1±6.3	
σ_{3p}^b					24.9±3.7	15.2±2.2
σ_t	72.8	58.7	56.5	42.8	34.8	20.8
σ_t^d	70.1±14.0	54.0±10.8	50.9±11.8	37.0±7.4	30.5±7.0	24.5±4.9
σ_t^a	99.9±42.0	60.7±25.5		47.6±20.0	34.3±14.4	
σ_t^c	85.2±10.2	73.9±8.9				

C. Integrated and total cross sections

In Table III we present the integrated elastic σ_{3s}, integrated $3\,^2S - 3\,^2P$, inelastic σ_{3p}, and total σ_t cross sections resulting from our 3CCO calculation together with various experimental estimates. The 3CCO σ_{3s} is considerably lower than experiment at 10 eV, but the agreement improves for higher energies. The 3CCO σ_{3p} is in complete agreement with both experimental estimates at all energies. The 3CCO total cross sections σ_t, calculated via the optical theorem, are in excellent agreement with the measurements of Kwan *et al.* across all energies. This is particularly pleasing at the low energies where our estimate of σ_{3s} is considerably less than experiment, but is consistent with the total-cross-section measurements.

IV. CONCLUSIONS

The differential cross section is sometimes considered to be one of the least sensitive parameters of the complete set which describes a scattering process. This is due to the fact that the differential cross section depends only on the absolute value of the T matrix. Furthermore the effects of spin are averaged. Note however that the differential cross section is an absolute number which may vary over many orders of magnitude as a function of angle, whereas spin- and phase-dependent parameters are ratios. Spin asymmetries have been recently measured by the NIST group (Celotta, Kelley, Lorentz, McClelland, and Scholten) and will soon be available. As we believe that our 3CCO calculations have achieved sufficient agreement with experimental differential cross sections, we will further test our theory against their spin- and phase-dependent parameters, as well as other currently available data.

ACKNOWLEDGMENTS

We thank Dr. S. R. Lorentz and Professor T. M. Miller for making available their experimental data to us prior to publication, and Dr. P. J. O. Teubner for some useful discussions of our results. We would like to acknowledge support from the Australian Research Council. One of us (D.A.K.) acknowledges financial support from The Flinders University of South Australia.

[1] I. Bray, D. A. Konovalov, and I. E. McCarthy, Phys. Rev. A **43**, 1301 (1991).
[2] I. Bray, D. A. Konovalov, and I. E. McCarthy, J. Phys. B **24**, 2083 (1991).
[3] I. Bray, D. A. Konovalov, and I. E. McCarthy, Phys. Rev. A **43**, 5878 (1991).
[4] I. Bray, D. H. Madison, and I. E. McCarthy, Phys. Rev. A **41**, 5916 (1990).
[5] I. Bray, D. A. Konovalov, and I. E. McCarthy, this issue, Phys. Rev. A **44**, 7830 (1991).
[6] L. V. Chernysheva, N. A. Cherepkov, and V. Radojevic, Comput. Phys. Commun. **11**, 57 (1976).
[7] C. Froese-Fischer, *The Hartree-Fock Method for Atoms* (Wiley, New York, 1977).
[8] L. V. Chernysheva, N. A. Cherepkov, and V. Radojevic, Comput. Phys. Commun. **18**, 87 (1979).
[9] J. Mitroy, I. E. McCarthy, and A. T. Stelbovics, J. Phys. B **20**, 4827 (1987).
[10] I. E. McCarthy and A. T. Stelbovics, Phys. Rev. A **28**, 2693 (1983).
[11] Steven R. Lorentz and Thomas M. Miller (unpublished).
[12] S. K. Srivastava and L. Vušković, J. Phys. B **13**, 2633 (1980).
[13] P. J. O. Teubner, S. J. Buckman, and C. J. Noble, J. Phys. B **11**, 2345 (1978).
[14] S. J. Buckman and P. J. O. Teubner, J. Phys. B **12**, 1741 (1979).
[15] P. J. O. Teubner, J. L. Riley, M. J. Brunger, and S. J. Buckman, J. Phys. B **19**, 3313 (1986).
[16] L. J. Allen, M. J. Brunger, I. E. McCarthy, and P. J. O. Teubner, J. Phys. B **20**, 4861 (1987).
[17] C. K. Kwan, W. E. Kauppila, R. A. Lukaszew, S. P. Parikh, T. S. Stein, Y. J. Wan, and M. S. Dababneh, Phys. Rev. A **44**, 1620 (1991).
[18] I. V. Hertel and K. J. Ross, J. Phys. B **2**, 285 (1969).
[19] A. Kasdan, T. M. Miller, and B. Bederson, Phys. Rev. A **8**, 1562 (1973).